SUPPLEMENTAL INFORMATION

SUPPLEMENTAL EXPERIMENTAL PROTOCOLS

Data Analysis. Activation parameters were estimated from the peak I-V curves obtained for each channel combination and are reported as the mean of individual measurements ± S.E.M. Briefly, the I-V relationships were normalized to the maximum amplitude and were fitted to a Boltzmann equation with $E_{0,5,act}$ being the mid-potential of activation as described elsewhere (1-3). The free energy of activation was calculated using the mid-activation potential by equation

$$\Delta G_{act} = z \cdot F \cdot E_{0.5,act} \quad (1)$$

The estimation of $E_{0,5,act}$ using non stationary measurements rests upon the assumption that the transition to the open state is much faster than the transition to the inactivated state. The measure of ΔG_{act} yields an estimation of the free energy differences between closed (C) and open (O) states such that:

$$\Delta G_{act} = zFE_{0,5,act} = -RT \ln([O]/[C]) \quad (2)$$

where [O]/[C] is the probability of finding the channel in the open state over the probability of finding the channel in the closed state, z is the effective charge at zero voltage, and T, F, and R have their usual meaning (4). Changes in ΔG_{act} can thus be interpreted as a modification of the ratio between the open and the closed states.

Deactivation time constants of whole-cell current traces were estimated with the predefined equations in Clampfit 10 that uses the Chebyshev routine and a 4-pt smoothing filter with a single exponential function. The r50 ratio is defined as the ratio of peak whole-cell currents remaining 50 ms later (I_{50ms} / I_{Peak}) as has been used in previous papers to estimate inactivation kinetics of $Ca_V2.3$ (3). The voltage-dependence of inactivation was obtained after a series of 5 sec prepulses that varied from -140 to +30 mV at a frequency of 0.02 Hz with $E_{0.5,inact}$ being the mid-potential of inactivation (1-3). Most mutations inactivated completely within the 5-s pulse with less than 1% of the peak currents remaining at the end of the inactivating pulse. However the phrase "isochronal inactivation" is more accurate when estimating the voltage-dependence of inactivation of the I701G mutant that displayed 15% residual currents.

Double mutant cycle analysis. The coupling coefficient Ω was calculated with the equation:

$$\Omega = \frac{K_{act,WT} \cdot K_{act,double}}{K_{act,S4S5} \cdot K_{act,S6}} \quad (3)$$

in which WT refers to the WT protein, S4S5 and S6 to the single S4S5 and S6 mutants respectively and double refers to the double mutant channel (S4S5 / S6) (5). The K_{act} affinity constants were obtained with the equation

$$K_{act} = \exp(\Delta G_{act} / RT) \quad (4)$$

This equation, combined to equation (2), was used to express the coupling coefficient as a function of the individual ΔG_{act}. When multiplied by RT, this coefficient becomes the interaction energy, $\Delta\Delta G_{interact}$:

$$\Delta\Delta G_{interact} = RT \cdot \ln(\Omega) = (\Delta G_{act,WT} + \Delta G_{act,S4S5;S6}) - (\Delta G_{act,S4S5} + \Delta G_{act,S6}) \quad (5)$$

The experimental error on $\Delta\Delta G_{interact}$ was propagated in a linear fashion. Any ln Ω value that tends to 0 suggests that the activation energies are purely additive and the residues are not interacting.

Homology modeling of $Ca_V2.3$. An analysis based on the SAMT02 algorithm (6) confirmed Kv1.2 as a suitable template to model the S4S5 linker and S6 segments of domain II of $Ca_V2.3$. The identity of Kv1.2 with $Ca_V2.3$ at the primary sequence was 25.9% for IIS6 and 31.6% for the IIS4-S5 linker. The primary sequence of each of the IIS4-S5 and IIS6 segment of $Ca_V2.3$ was aligned with the similar regions in Kv1.2 by using T-COFFEE (7) using the full alignment shown below. The score for the alignment of the distal IIS6 was higher than for the beginning of the IIS6 segment. The model for the S6 segments was described in details in (3) and the same procedure was used to build the model including the IIS4-S5 linker. The computer-based molecular model of $Ca_V2.3$, going from IIS4 helix to the end of IIS6 was obtained with Modeller 9v4 (http://salilab.org/modeller) using the molecular coordinates of Kv1.2 (2A79.pdb). Fifty models were generated. We used the model with the lowest internal energy.

T-COFFEE Output

```
CLUSTAL FORMAT for T-COFFEE Version_8.14 [http://www.tcoffee.org]

Kv1.2    LRVIRLVRVFRIFKLSRHSKGLQILGQTLKASMRELGLLIFFL--------FIGVILFSSAVYFAEAD-
Cav2.3   ISVLRALRLLRIFKITKYWASLRNLVVSLMSSMKSIISLLFLLFLFIVVFALLGMQLFGGRFNFND—G

Kv1.2    -ERDSQFPSIPDAFWWAVVSMTTVGYGDMVPTTIGGK—---------IVGSLCAIAGVLTIALPVPVIV
Cav2.3   TPSANFDTFPAAIITVFQILTGEDWNEVMYNGIRSQGGVSSGMWSAIYFIVLTLFGNYTLLNVFLAIAV

Kv1.2    SNFNYF--------------------YHRET*
Cav2.3   DNLANAQELTKDEQEEEEAFNQKHALQKAKEV*
```

SUPPLEMENTAL RESULTS

Intradomain interactions in Domains I, III, IV

As $\Delta\Delta G_{interact}$ were quite high within Domain II, we aimed to test the cooperativity within Domains I, III, and IV. Residues predicted to be aligned with L596 in Domains I, III, and IV were mutated to glycine and their biophysical properties were characterized. As shown in Table I, I214G (Domain I), V1281G (Domain III), and F1599G (Domain IV) were not significantly different from the wild-type channel. Unfortunately, double glycine mutants with respectively V349G (IS6), L1420G (IIIS6) and V1720G (IVS6) failed to yield functional channels.

SUPPLEMENTAL LEGENDS

SUPPLEMENTAL FIGURE S1. The SAMT02 algorithm was run from P562 (IIS4) to A618 (IIS5S6 linker) of $Ca_V2.3$. The helical probability, given by the DSSP_EHL alphabet prediction of the SAM-T02 algorithm, is plotted against the residue number. The simulation for the wild-type channel (black) predicts an α-helical conformation for IIS4S5. As seen, introducing single glycine residues was not predicted to alter the secondary structure of IIS4S5.

SUPPLEMENTAL FIGURE S2. Normalized current-voltage relationships of double IIS4S5/I701G mutantswere obtained by fitting the experimental data to a Boltzmann equation. In each graph, $Ca_V2.3$ wt is displayed as a dashed line, blue squares show the single IIS4S5 glycine mutant, red circles represent I701G, and green diamonds correspond to the double IIS4S5/I701G mutant. Numerical values of the activation properties are provided in Table II.

SUPPLEMENTAL FIGURE S3. Normalized current-voltage relationships of double L596G/IIS6 mutants were obtained by fitting the experimental data to a Boltzmann equation. In each graph, $Ca_V2.3$ wt is displayed as a

dashed line, L596G mutant as blue squares, the single IIS6 glycine mutants in red circles and the double L596G/IIS6 mutants in green diamonds. Numerical values of the activation properties are provided in Table II.

SUPPLEMENTAL FIGURE S4. A. Whole-cell current traces for V593G, I701G, and V593G/I701G co-expressed with $Ca_V\alpha2b\delta$ and $Ca_V\beta3$ were recorded in 10 mM Ba^{2+}. Holding potential was -120 mV throughout. **B.** Normalized current-voltage relationships for $Ca_V2.3$ wt (dashed line), V593G (blue squares), I701G (red circles) and V593G/I701G (green diamonds) were obtained by fitting the experimental data to a Boltzmann equation. **C.** Gating currents were measured with the cut-open oocyte technique. The voltage-dependence of the gating charge or $V_{0.5,Q}$ values were obtained from fitting the gating currents with a single Boltzmann equation as described in "Experimental Procedures". $V_{0.5,Q}$ values were 6 ± 1 mV (n = 19) for $Ca_V2.3$ wt, -20 ± 1 mV (n = 15) for I701G, 1 ± 1 mV (n = 4) for V593G, and -24 ± 1 mV (n = 9) for V503G/I701G.

SUPPLEMENTAL FIGURE S5. A. Whole-cell current traces are shown for M597G, I701G, and M597G/I701G in the presence of $Ca_V\alpha2b\delta$ and $Ca_V\beta3$. Currents were recorded in 10 mM Ba^{2+} from a holding potential of -120 mV. **B.** Normalized current-voltage relationships for $Ca_V2.3$ wt (dashed line), M597G (blue squares), I701G (red circles) and M597G/I701G (green diamonds) obtained by fitting the experimental data to a Boltzmann equation. **C.** Gating currents were measured with the cut-open oocyte technique. The voltage-dependence of the gating charge or $V_{0.5,\ Q}$ values were obtained from fitting the traces with a single Boltzmann equation as described in "Experimental Procedures". $V_{0.5,\ Q}$ values were 6 ± 1 mV (n = 19) for $Ca_V2.3$ wt, -20 ± 1 mV (n = 15) for I701G, -8 ± 1 mV (n = 4) for M597G, and -20 ± 1 mV (n = 4) for M597G/I701G.

SUPPLEMENTAL TABLE S1. BIOPHYSICAL PROPERTIES OF IIS6 MUTANTS IN $Ca_V2.3$

$Ca_V2.3/\alpha2\delta/\beta3$ 10 mM Ba^{2+}	Activation		Inactivation			Deactivation
	$E_{0.5.act}$ (mV)	ΔG_{act} (kcal mol^{-1})	$E_{0.5.inact}$ (mV)	ΔG_{inact} (kcal mol^{-1})	R50 at 10 mV	max τ deact (ms)
$Ca_V2.3$ wt	-6.7 ± 0.4 (108)	-1.0 ± 0.1	-63.5 ± 0.6 (74)	-4.3 ± 0.1	0.41 ± 0.02 (41)	1.3 ± 0.2 (10)
L699G	-19 ± 1 (13)**	-2.0 ± 0.2**	-62 ± 1 (7)	-4.1 ± 0.4	0.64 ± 0.01 (5)**	2.4 ± 0.2 (5) *
A700G	-14.1 ± 0.9 (10)**	-1.5 ± 0.1	-80 ± 1 (5)**	-2.7 ± 0.1**	0.69 ± 0.04 (10)**	1.2 ± 0.1 (5)
I701G	-45 ± 2 (24)**	-4.7 ± 0.3**	-84 ± 1 (12)**	-7 ± 1 **	0.82 ± 0.04 (24) **	30 ± 2 (6)**
A702G	-11 ± 1 (20) **	-1.2 ± 0.1	-62 ± 1 (20)	-3.2 ± 0.2 **	0.67 ± 0.01 (20) **	1.0 ± 0.2 (5)
V703G	-29 ± 1 (15) **	-3.6 ± 0.2 **	-81 ± 1 (7) **	-3.2 ± 0.1 **	0.68 ± 0.02 (15) **	0.8 ± 0.1 (5) **
D704G	-17 ± 1 (5) **	-1.9 ± 0.1	-71 ± 1 (5) *	-4.3 ± 0.1	0.61± 0.03 (5) *	1.2 ± 0.2 (5)

SUPPLEMENTAL TABLE S1. Biophysical parameters of $Ca_V2.3$ wild-type and IIS6 mutant channels were estimated with $Ca_V\alpha2b\delta$ and $Ca_V\beta3$ in the presence of a 10 mM Ba^{2+} solution as described elsewhere (1,2,8). The voltage-dependence of inactivation was determined from the peak currents after 5 s depolarizing pulses from a holding potential of -120 mV. Activation properties ($E_{0.5,act}$ and z) were estimated from the mean I-V relationships and fitted to a Boltzmann equation where z is the slope factor. The data are shown with the mean ± S.E.M. of the individual experiments and the number of experiments appears in parentheses. * $p < 0.01$ **; $p < 0.001$ as compared with $Ca_V2.3$ wt.

SUPPLEMENTAL TABLE S2. INACTIVATION GATING OF THE DOMAIN II DOUBLE MUTANTS IN $Ca_V2.3$

$Ca_V2.3/\alpha2\delta/\beta3$ 10 mM Ba^{2+}	Inactivation				
	$E_{0.5.inact}$ (mV)	ΔG_{inact} (kcal mol^{-1})	r50 at +10 mV	ln Ω	$\Delta\Delta G_{interact}$ (kcal mol^{-1})
L592G / I701G	-87 ± 1 (4) **	-5.6 ± 0.5 **	0.90 ± 0.02 (4) **	1 ± 1	0.4 ± 0.7
V593G / L699G	-64 ± 2 (5)	-3.4 ± 0.2 *	0.67 ± 0.04 (5) **	0 ± 2	0 ± 1
V593G / A700G	-97 ± 1 (4) **	-5.4 ± 0.4 *	0.62 ± 0.01 (4) *	-6 ± 2	-3 ± 1
V593G / I701G	-87 ± 1 (5) **	-5.0 ± 0.2	0.88 ± 0.01 (5) **	0 ± 2	0 ± 1
V593G / A702G	-91 ± 1 (5) **	-3.15 ± 0.05 **	0.53 ± 0.05 (5)	-1 ± 2	-1 ± 1
V593G / V703G	-71 ± 1 (5) *	-3.3 ± 0.2 *	0.61 ± 0.03 (5) **	-2 ± 2	-1 ± 1
V594G / L699G	-57 ± 3 (5)	-4.4 ± 0.3	0.70 ± 0.03 (5) **	-4 ± 2	-2.1 ± 0.9
V594G/ A700G	-74 ± 1 (4) **	-4.1 ± 0.1	0.68 ± 0.01 (4) **	-5 ± 1	-3.2 ± 0.4
V594G / I701G	-54 ± 2 (3) *	-4.1 ± 0.5	0.88 ± 0.07 (5) **	0 ± 2	0 ± 1
V594G / A702G	-50 ± 3 (6) **	-3.6 ± 0.2 *	0.62 ± 0.03 (6) **	-4 ± 1	-2.2 ± 0.6
V594G / V703G	-58 ± 1 (5)	-3.5 ± 0.3	0.80 ± 0.02 (5) **	-4 ± 1	-2.1 ± 0.6
V594G / D704G	-62 ± 1 (5)	-4.3 ± 0.2	0.57 ± 0.04 (5) *	-3 ± 1	-1.8 ± 0.5
S595G / L699G	-51 ± 2 (4) **	-3.6 ± 0.3	0.88 ± 0.01 (5) **	-2 ± 2	-1.3 ± 0.9
S595G / A700G	-68 ± 1 (5)	-3.8 ± 0.2	0.85 ± 0.02 (6) **	-5 ± 1	-2.9 ± 0.5
S595G / I701G	-93 ± 1 (4) **	-4.7 ± 0.1	0.86 ± 0.01 (5) **	-1 ± 1	-0.7 ± 0.6
S595G / A702G	-48 ± 1 (5) **	-3.4 ± 0.2 *	0.82 ± 0.01 (5) **	-3 ± 1	-2 ± 0.6
S595G / V703G	-54 ± 3 (4) *	-2.7 ± 0.1 **	0.90 ± 0.02 (3) **	-2 ± 1	-1.3 ± 0.4
L596G / L699G	-57 ± 1 (5)	-3.0 ± 0.2 **	0.60 ± 0.02 (5) *	2 ± 2	1.5 ± 0.9
L596G / A700G	-80 ± 1 (5) **	-4.7 ± 0.1	0.70 ± 0.02 (5) **	-2 ± 1	-1.6 ± 0.5
L596G / I701G	-102 ± 2 (5) **	-5.1 ± 0.4	0.87 ± 0.02 (5) **	1± 2	1 ± 1

L596G / A702G	-64 ± 1 (5)	-4.5 ± 0.2	0.70 ± 0.01 (5) **	-1 ± 1	-0.9 ± 0.7
L596G / V703G	-72 ± 2 (5) **	-3.7 ± 0.1	0.77 ± 0.01 (5) **	0 ± 1	-0.1 ± 0.5
L596G / D704G	-68 ± 1 (5)	-4.3 ± 0.2	0.64 ± 0.03 (5) **	1 ± 1	0.4 ± 0.6
M597G / L699G	-75 ± 2 (5) **	-4.3 ± 0.7	0.58 ± 0.04 (5) *	-2 ± 2	-1 ± 1
M597G / A700G	-100 ± 1 (5) **	-4.5 ± 0.1	0.61 ± 0.02 (5) **	-4 ± 1	-2.5 ± 0.5
M597G / I701G	-59 ± 2 (4)	-3.4 ± 0.3	0.58 ± 0.03 (5) *	3 ± 2	1.7 ± 0.9
M597G / A702G	-73 ± 1 (5) **	-3.7 ± 0.1	0.54 ± 0.02 (5)	-2 ± 1	-1.2 ± 0.6
M597G / V703G	-78 ± 1 (4) **	-2.9 ± 0.1 **	0.66 ± 0.03 (5) **	-1 ± 1	-0.4 ± 0.5
M597G / D704G	-90 ± 1 (5) **	-3.9 ± 0.2	0.38 ± 0.02 (5)	-1 ± 1	-0.3 ± 0.6
S598G / L699G	-53 ± 1 (5) **	-2.7 ± 0.1 **	0.54 ± 0.04 (5)	1 ± 1	0.5 ± 0.7
S598G / A700G	-86 ± 1 (5) **	-5.2 ± 0.4	0.61 ± 0.01 (5) **	-6 ± 1	-3.4 ± 0.7
S598G / I701G	-73 ± 2 (4) **	-4.3 ± 0.3	0.92 ± 0.02 (5) **	1 ± 1	0.6 ± 0.8
S598G / A702G	-63 ± 1 (5)	-4.1 ± 0.1	0.65 ± 0.01 (5) **	-3 ± 1	-1.8 ± 0.5
S598G / V703G	-77 ± 1 (4) **	-3.9 ± 0.1	0.65 ± 0.01 (5) **	-3 ± 1	-1.6 ± 0.4
S598G / D704G	-67 ± 1 (5)	-4.0 ± 0.2	0.35 ± 0.01 (5)	-1 ± 1	-0.6 ± 0.5
S599G / I701G	-69 ± 1 (4)	-4.2 ± 0.2	0.79 ± 0.06 (6) **	2 ± 1	1.4 ± 0.7
M600G / I701G	-86 ± 1 (5) **	-4.2 ± 0.2	0.82 ± 0.04 (5) **	3 ± 1	1.6 ± 0.7
K601G / I701G	-67 ± 1 (5)	-4.0 ± 0.1	0.89 ± 0.03 (4) **	1 ± 1	0.6 ± 0.6
S602G / I701G	-84 ± 1 (4) **	-4.5 ± 0.3	0.90 ± 0.02 (4) **	2 ± 1	1.4 ± 0.9

SUPPLEMENTAL TABLE S2. Inactivation gating properties of $Ca_V2.3$ double mutant channels were estimated with $Ca_V\alpha2b\delta$ and $Ca_V\beta3$ in the presence of a 10 mM Ba^{2+} solution as described elsewhere (1,2,8). The voltage-dependence of inactivation was determined from the peak currents after 5 s depolarizing pulses from a holding potential of -120 mV (-140 mV for L596G double mutants). The data are shown with the mean ± S.E.M. of the individual experiments and the number of experiments appears in parentheses. Ln Ω factor and $\Delta\Delta G_{interact}$ were calculated for double mutants as indicated in Experimental Procedures. * $p < 0.01$ **; $p < 0.001$ as compared with $Ca_V2.3$ wt.

SUPPLEMENTAL TABLE S3. ACTIVATION GATING PROPERTIES OF L589G/I701G IN $Ca_V2.3$

$Ca_V2.3/\alpha2\delta/\beta3$ 10 mM Ba^{2+}	Activation				Deactivation
	$E_{0.5.act}$ (mV)	ΔG_{act} (kcal mol^{-1})	ln(Ω)	$\Delta\Delta G_{interact}$ (kcal mol^{-1})	max τ deact (ms)
L589G	-12 ± 2 (5)	-1.2 ± 0.2	--	--	5 ± 2 (5)
L589G / I701G	-54 ± 1 (5) **	-5.0 ± 0.3 **	2 ± 1	1.1 ± 0.9	22 ± 2 (5) **

SUPPLEMENTAL TABLE S3. Activation gating properties of L589G and L589G/I701G mutants were estimated with $Ca_V\alpha2b\delta$ and $Ca_V\beta3$ in the presence of a 10 mM Ba^{2+} solution as described elsewhere (1,2,8). Activation properties ($E_{0.5,act}$ and z) were estimated from the mean I-V relationships from a holding potential of -100 mV and fitted to a Boltzmann equation where z is the slope factor. The data are shown with the mean ± S.E.M. of the individual experiments and the number of experiments appears in parentheses. Ln Ω factor and $\Delta\Delta G_{interact}$ were calculated for double mutants as indicated in Experimental Procedures with ΔG_{act} values (in kcal mol^{-1}) for I701G = -4.7 ± 0.3 (n=24). **; $p < 0.001$ as compared with $Ca_V2.3$ wt.

SUPPLEMENTAL TABLE S4. ACTIVATION GATING PROPERTIES OF L674G/I781G IN $Ca_V1.2$

$Ca_V1.2/\alpha2\delta/\beta3$ 10 mM Ba^{2+}	Activation				Deactivation
	$E_{0.5.act}$ (mV)	ΔG_{act} (kcal mol^{-1})	ln(Ω)	$\Delta\Delta G_{interact}$ (kcal mol^{-1})	max τ deact (ms)
$Ca_V1.2$ wt	-8.0 ± 0.4 (141)	-0.81 ± 0.04	--	--	1.1 ± 0.7 (18)
L674G	-20 ± 1 (5) **	-2.2 ± 0.3 **	--	--	1.5 ± 0.3 (5)
I781G	-31 ± 1 (15) **	-2.5 ± 0.1 **	--	--	10.6 ± 0.4 (6) **
L674G / I781G	-45 ± 2 (5) **	-4.8 ± 0.3 **	-2 ± 1	-0.9 ± 0.7	9.4 ± 0.8 (5) **

SUPPLEMENTAL TABLE S4. Activation gating properties of $Ca_V1.2$ wt, L674G, I781G and L674G/I781G mutants were estimated with $Ca_V\alpha2b\delta$ and $Ca_V\beta3$ in the presence of a 10 mM Ba^{2+} solution as described elsewhere (1,2,8). Activation properties ($E_{0.5,act}$ and z) were estimated from the mean I-V relationships from a holding potential of -100 mV and fitted to a Boltzmann equation where z is the slope factor. The data are shown with the mean ± S.E.M. of the individual experiments and the number of experiments appears in parentheses. Ln Ω factor and $\Delta\Delta G_{interact}$ were calculated for double mutants as

indicated in Experimental Procedures with ΔG_{act} values (in kcal mol^{-1}) for I701G = -4.7 ± 0.3 (n=24). **; p < 0.001 as compared with $Ca_V2.3$ wt.

SUPPLEMENTAL TABLE S5. ACTIVATION GATING PROPERTIES OF L603G/I712G IN $Ca_V2.1$

$Ca_V1.2/\alpha2\delta/\beta3$ 10 mM Ba^{2+}	Activation			
	$E_{0.5.act}$ (mV)	ΔG_{act} (kcal mol^{-1})	ln(Ω)	$\Delta\Delta G_{interact}$ (kcal mol^{-1})
$Ca_V2.1$ wt	-7 ± 1 (25)	-1.1 ± 0.1	--	--
L603G	-11 ± 1 (5) **	-1.7 ± 0.2 **	--	--
I712G	-43 ± 1 (7) **	-5.0 ± 0.2 **	--	--
L603G / I712G	-45 ± 1 (6) **	-5.2 ± 0.2 **	1 ± 1	0.4 ± 0.7

SUPPLEMENTAL TABLE S5. Activation gating properties of $Ca_V2.1$ wt, L603G, I712G and L603G/I712G mutants were estimated with $Ca_V\alpha2b\delta$ and $Ca_V\beta3$ in the presence of a 10 mM Ba^{2+} solution as described elsewhere (1,2,8). Activation properties ($E_{0.5,act}$ and z) were estimated from the mean I-V relationships from a holding potential of -100 mV and fitted to a Boltzmann equation where z is the slope factor. The data are shown with the mean ± S.E.M. of the individual experiments and the number of experiments appears in parentheses. Ln Ω factor and $\Delta\Delta G_{interact}$ were calculated for double mutants as indicated in Experimental Procedures with ΔG_{act} values (in kcal mol^{-1}) for I701G = -4.7 ± 0.3 (n=24). **; p < 0.001 as compared with $Ca_V2.3$ wt.

Reference List

1. Berrou, L., Bernatchez, G., and Parent, L. (2001) *Biophys. J.* **80,** 215-228
2. Berrou, L., Dodier, Y., Raybaud, A., Tousignant, A., Dafi, O., Pelletier, J. N., and Parent, L. (2005) *J. Biol. Chem.* **280,** 494-505
3. Raybaud, A., Baspinar, E. E., Dionne, F., Dodier, Y., Sauve, R., and Parent, L. (2007) *J Biol. Chem.* **282(38),** 27944-27952
4. Yifrach, O. and MacKinnon, R. (2002) *Cell.* **111,** 231-239
5. Horovitz, A. (1996) *Fold. Des.* **1,** R121-R126
6. Karplus, K., Karchin, R., Draper, J., Casper, J., Mandel-Gutfreund, Y., Diekhans, M., and Hughey, R. (2003) *Proteins.* **53 Suppl 6:491-6.,** 491-496
7. Notredame, C., Higgins, D. G., and Heringa, J. (2000) *J. Mol. Biol.* **302,** 205-217
8. Berrou, L., Klein, H., Bernatchez, G., and Parent, L. (2002) *Biophys. J* **83,** 1429-1442

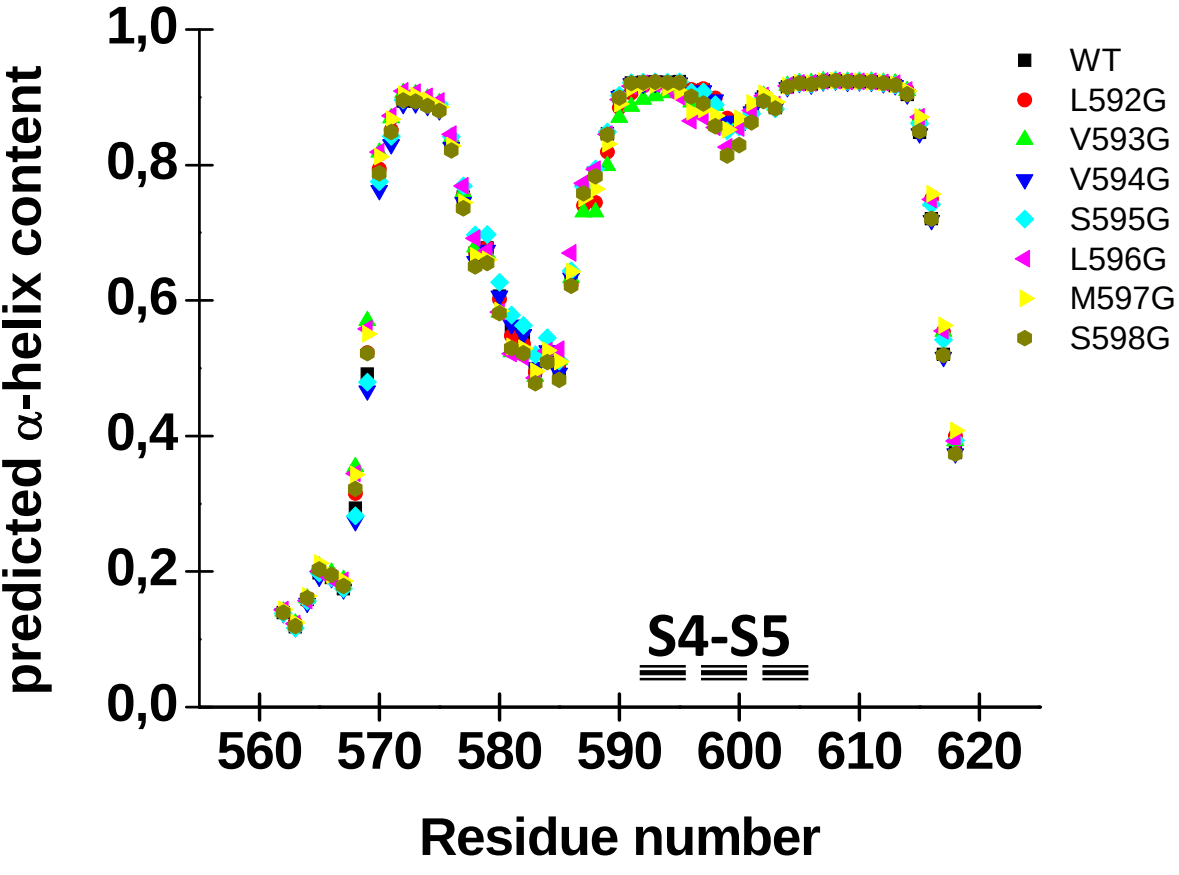

Suppl Figure S1

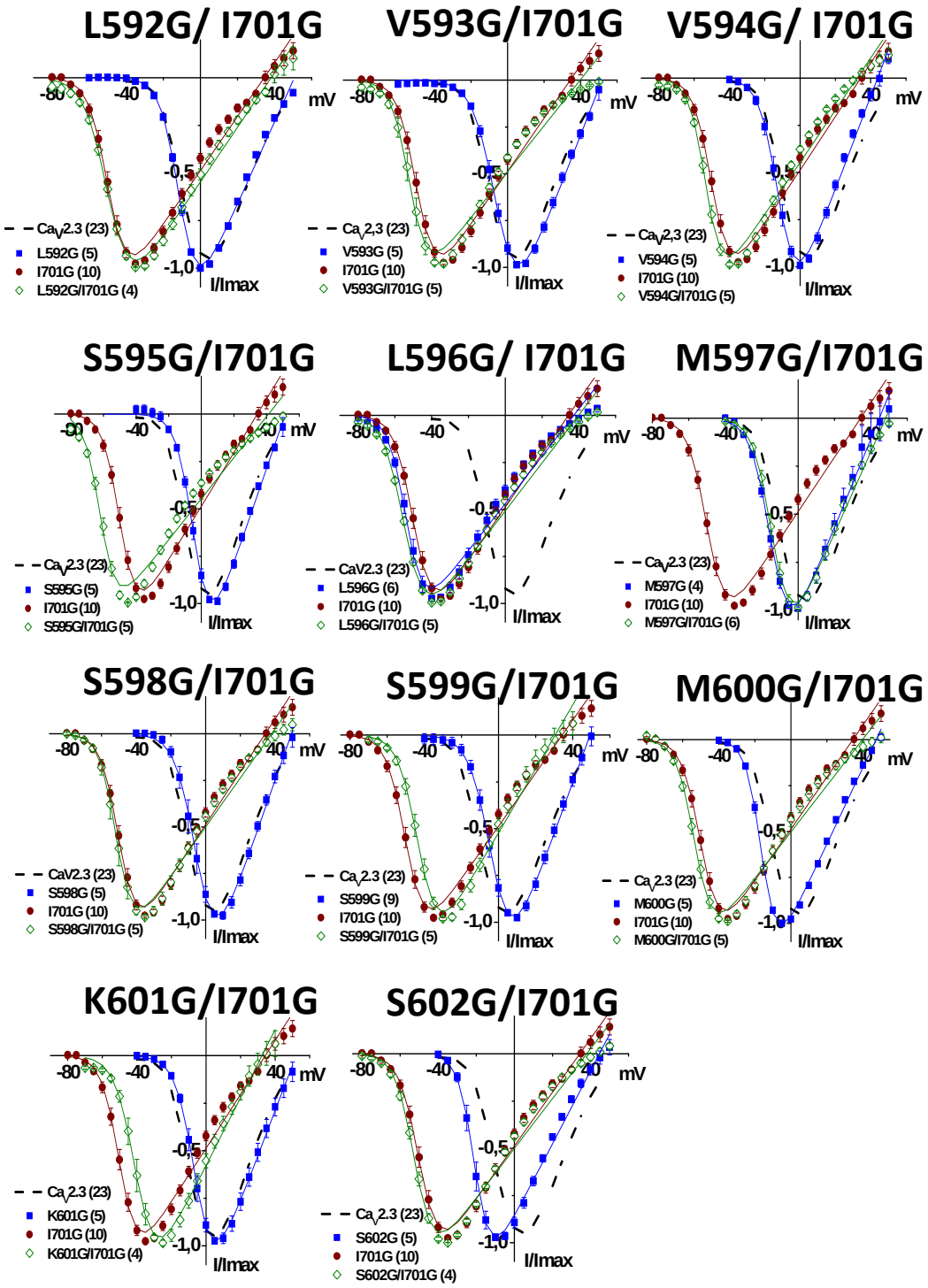

Suppl Figure S2

L596G / L699G

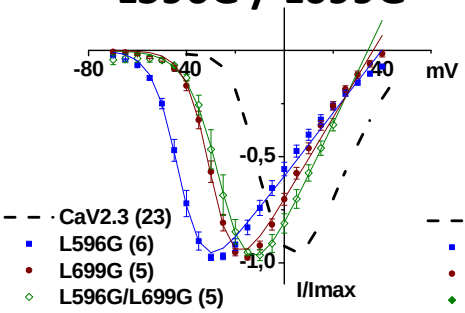

L596G/ A700G

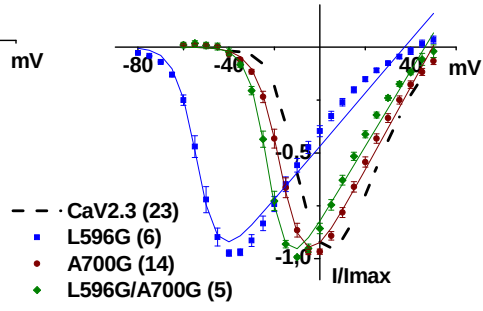

L596G / I701G

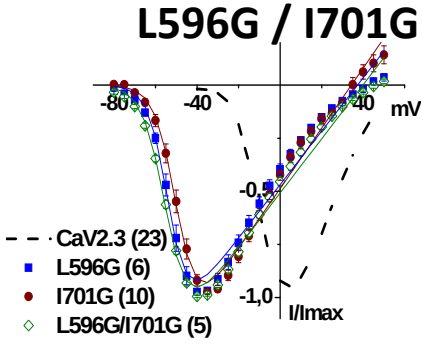

L596G /A702G

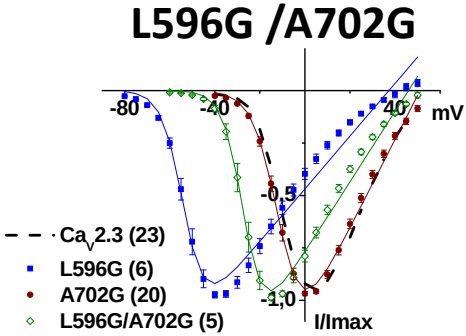

L596G /V703G

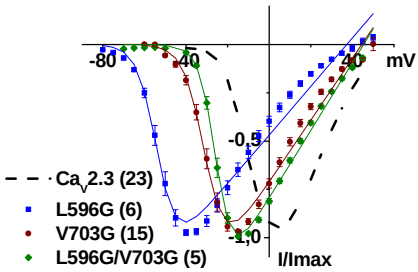

L596G /D704G

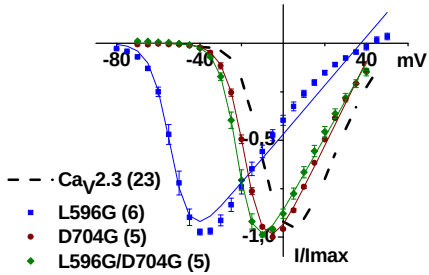

Suppl Figure S3

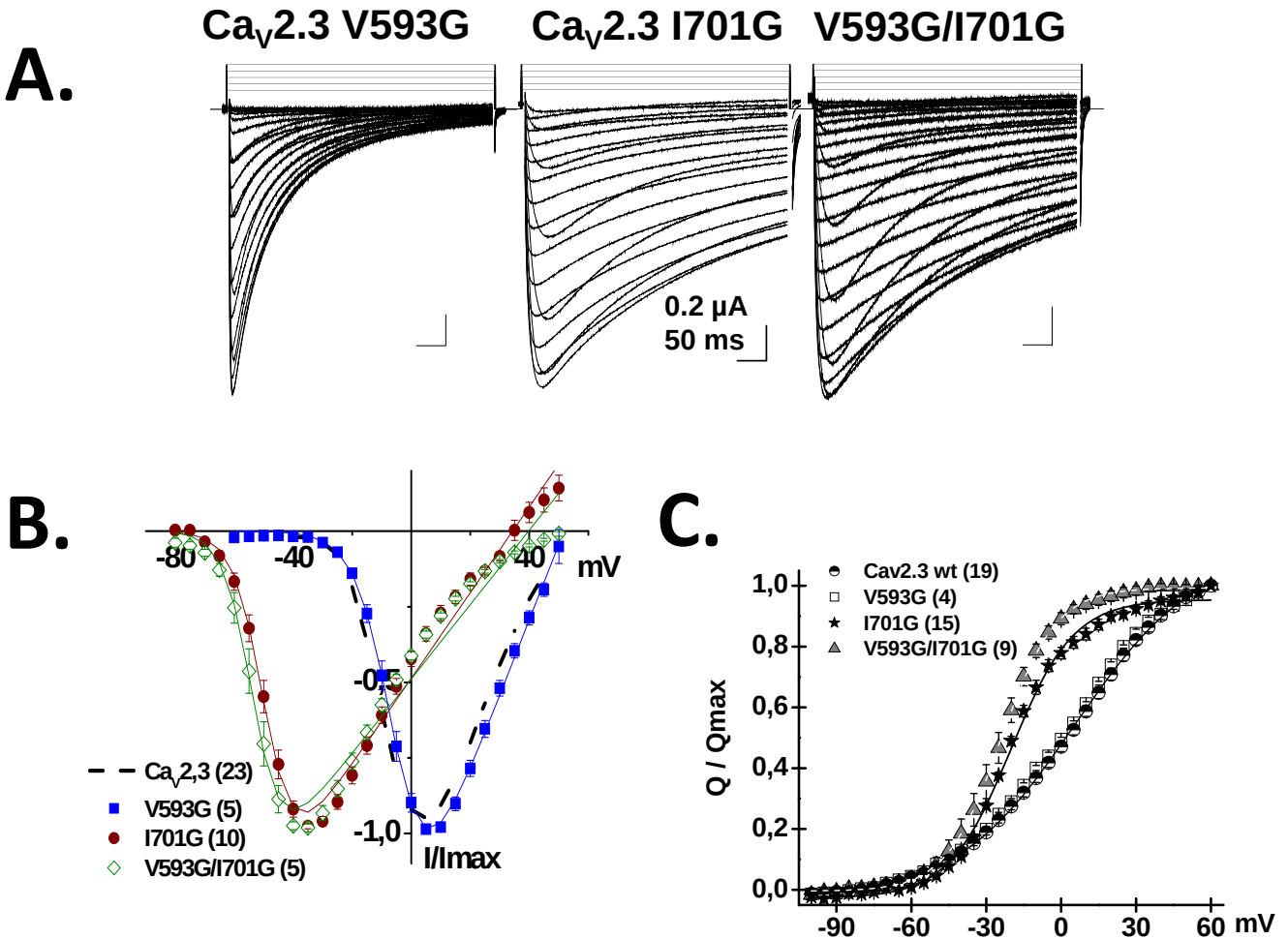

Suppl Figure S4

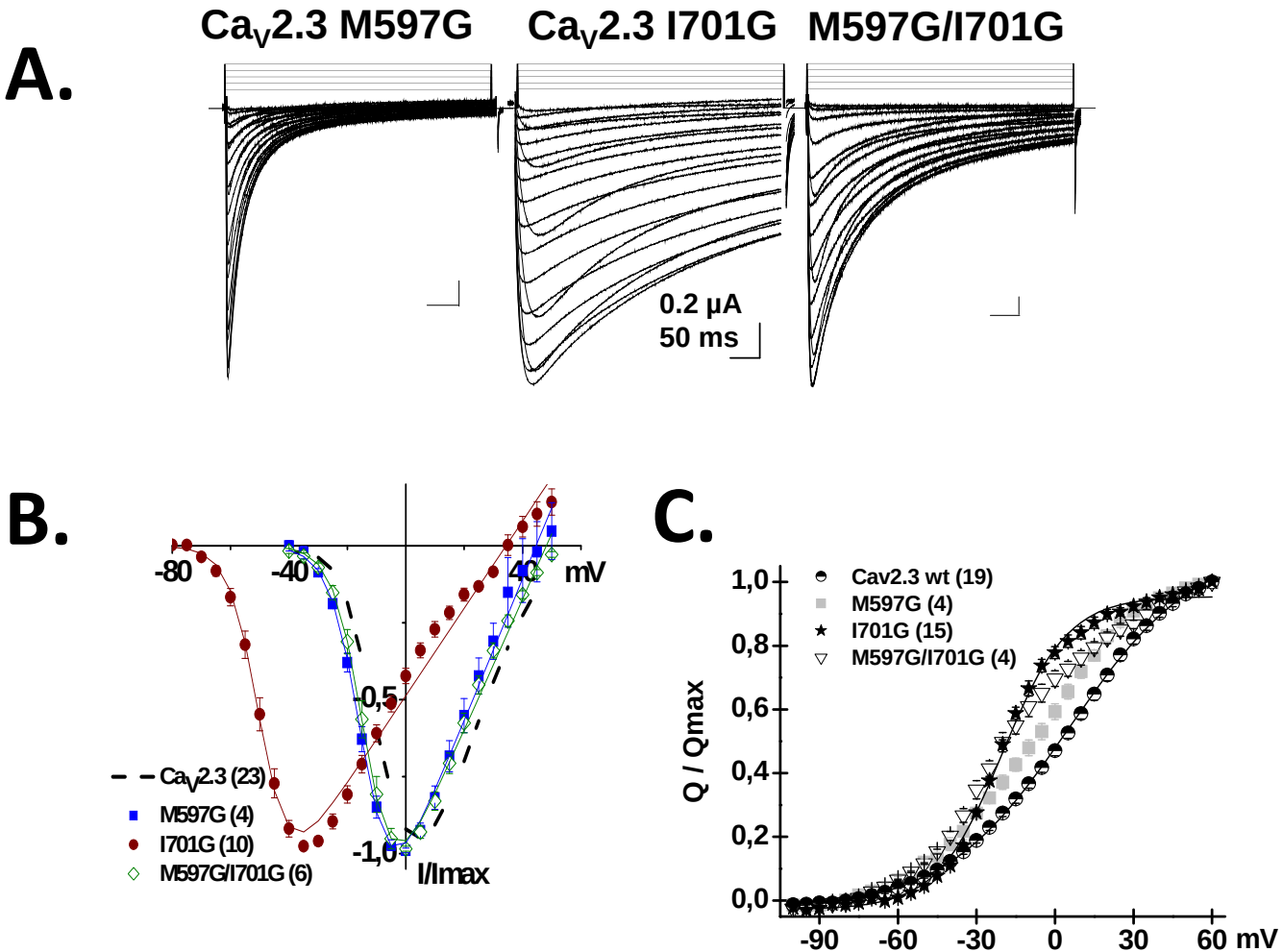

Suppl Figure S5